New Numerical Interface Scheme for the Kurganov-Tadmor Second Order Method

Pablo Esteban Montes[1,*], Oscar Reula[1]

[1] *Facultad de Matemática, Astronomía y Física (IFEG - CONICET), Universidad Nacional de Córdoba, Cordoba, Argentina*

Abstract. In this paper we develop a scheme that allows us to transmit shock discontinuities across numerical interfaces using the Kurganov-Tadmor (KT) second order method [1]. The scheme works by lowering the local order of convergence near the interface. We find that our interface scheme maintains the second order global convergence, while increasing the numerical dissipation. Analysis of the two dimensional Euler problem shows that shock discontinuities are correctly propagated across interfaces, regardless of the relative orientation between them. We also find that instabilities can be triggered across interfaces in the highly demanding Gresho vortex problem.

AMS subject classifications: 52B10, 65D18, 68U05, 68U07

Key words: multigrid method, conservative method, numerical interface, Kurganov-Tadmor method.

1 Introduction

Many systems of interest have a non-trivial topology that cannot be covered by a single computational domain in a smooth way. This leads to the need of multiple coordinate patches to cover the domain of integration. One approach in the numerical solution of such systems is to use multi-block methods. In these, a domain of dimension n is divided in several non-overlaping subdomains joined together by surfaces of dimension $n-1$ called interfaces. Each subdomain is then discretized and evolved in parallel, and the interfaces become regions that must be specially treated to allow the transmission of waves between grids.

The treatment of this interfaces is generally well understood for smooth solutions in which finite differences can be applied, but not so when shock discontinuities are involved. We are interested in systems of equations that allow the formation of shock waves; in particular, we focus on systems of conservation laws of the form

*Corresponding author.

$$\frac{\partial}{\partial t}u+\sum_j \frac{\partial}{\partial x_j}F^j(u)=0, \quad u|_{\partial\Omega,t=0}=u_0, \tag{1.1}$$

where u is a vector of conserved quantities, F^j are flux functions for each coordinate and Ω the domain of integration.

The non existence of a spatial derivative for the exact solution in the shock region translates to spurious oscillations of the numerical solution due to the Gibbs phenomena when finite differences are applied. Furthermore, the abrupt change of the numerical solution in the span of a few grid points makes for an extra challenge when interfaces between domains are involved.

Conservative methods try to avoid this oscillations by working with the weak formulation of (1.1), and can allow high orders of convergence in the smooth parts of the solution while keeping good accuracy near shock discontinuities. Unfortunately, there is not much development in ways to threat numerical interfaces for this kind of methods.

We are interested in a simple interface method that requires minimal communication between grids to implement in a high performance computing multiblock numerical relativity code, where the different multigrids are not aligned. In this work we develop a simple interface treatment for the second order Kurganov-Tadmor (KT) conservative method [1], based on it's first order formulation, that allows the transmission of shocks while maintaining the global order of convergence.

This paper is organized as follows: First we give a brief overview of the KT method and its total variation diminishing property (TVD). Then we introduce our interface method and show that the TVD property is maintained. After that, we show how the second order of convergence is maintained in the one dimensional case and shock discontinuities and waves are completely transmitted through interfaces without loss of speed or phase. Finally, we show results for the implementation of this interface for the two dimensional Euler equations.

2 Kurganov-Tadmor method

In this section we make a quick overview of the semi-discrete formulation of the KT method. More information can be found in [1].

We start with a simple one dimensional problem of the form

$$\frac{\partial u}{\partial t}(x,t)+\frac{\partial f(u)}{\partial x}(x,t)=0 \quad (x,t)\in[0,\infty)\times[0,\infty), \tag{2.1}$$

where u is vector of conserved quantities and f a convective flux.

We start by discretizing the spatial dimension in equal intervals of width Δx, and denote $x_j \doteq j\Delta x$. The cell average of u at grid point j is then defined as

$$\overline{u}_j(t) = \frac{1}{\Delta x}\int_{x_{(j-\frac{1}{2})}}^{x_{(j+\frac{1}{2})}} u(\xi,t)\,d\xi. \tag{2.2}$$

We can now combine (2.1) and (2.2) to obtain an equivalent weak formulation of the conservation law,

$$\frac{\partial \overline{u}}{\partial t}(x,t) = f\left(u(x_{j-1/2},t)\right) - f\left(u(x_{j+1/2},t)\right). \tag{2.3}$$

From now onwards we denote $v_j(t)$ as the numerical approximation of $\overline{u}(x_j,t)$. Conservative methods evolve the averages of the solution in small intervals, and thus need to approximate the intermediate values $v_{j\pm1/2}$. The main difference among schemes lies on the way that these intermediate values are approximated.

The semidiscrete KT method takes the conservative form

$$\frac{d}{dt}v_j(t) = -\frac{H_{j+1/2}(t) - H_{j-1/2}(t)}{\Delta x}, \tag{2.4}$$

$$H_{j+1/2}(t) := \frac{f(v^+_{j+1/2}(t)) + f(v^-_{j+1/2}(t))}{2} - \frac{a_{j+1/2}(t)}{2}\left[v^+_{j+1/2}(t) - v^-_{j+1/2}(t)\right], \tag{2.5}$$

$$v^+_{j+1/2}(t) = v_{j+1}(t) - \frac{\Delta x}{2}(v_x)_{j+1}(t) \quad v^-_{j+1/2}(t) = v_j(t) + \frac{\Delta x}{2}(v_x)_j(t), \tag{2.6}$$

where $(v_x)_j$ is some approximation of the spatial derivative of v and $a_{j+1/2}(t)$ the maximum propagation speed of the solution between $v^-_{j+1/2}(t)$ and $v^+_{j+1/2}(t)$,

$$a_{j+1/2}(t) = \max\left(\rho\left(\left|\frac{\partial f}{\partial v}\left(v^+_{j+1/2}(t)\right)\right|\right), \rho\left(\left|\frac{\partial f}{\partial v}\left(v^-_{j+1/2}(t)\right)\right|\right)\right), \tag{2.7}$$

and $\rho(\frac{\partial f}{\partial v}(v))$ represents the eigenvalues of the matrix $\frac{\partial f}{\partial v}(v)$.

A good starting point to understand this equation is setting $(v_x)_j = 0$. This assumption gives us the first order KT method, which can be expressed in the dissipative form

$$\begin{aligned}\frac{d}{dt}(v_j) = &-\frac{1}{2\Delta x}\left(f(v_{j+1}) - f(v_{j-1})\right) + \\ &\frac{1}{2\Delta x}\left(a_{j+1/2}(v_{j+1} - v_j) - a_{j-1/2}(v_j - v_{j-1})\right).\end{aligned} \tag{2.8}$$

While the first term in the RHS corresponds to the approximation of the numerical flux, the second one corresponds to a numerical dissipation. Because $(v_x)_j = 0$, our numerical approximation is piecewise constant in the intervals $x_{j-1/2}, x_{j+1/2}$. In contrast, the second order KT method is piecewise linear in those same intervals.

The approximation of the derivative, v_x, is chosen as to preserve the *total variation diminishing* property (TVD) [†] of the solutions to the scalar problem. This property is valid for the exact solutions and it ensures that no new extrema are created in the evolution of the numerical solution, thus preventing spurious oscillations near shock discontinuities [2]. The preservation of this property also requires the use of special temporal integrators [3].

The following choice for v_x satisfies the TVD property [4].

$$(v_x)_j = \text{minmod}\left(\theta\frac{v_j - v_{j-1}}{\Delta x}, \frac{v_{j+1} - v_{j-1}}{2\Delta x}, \theta\frac{v_{j+1} - v_j}{\Delta x}\right), \tag{2.9}$$

with the function minmod defined as

$$\text{minmod}(x_1, x_2, x_3, ...) = \begin{cases} \max(x_j) & \text{if } x_j > 0 \,\forall j, \\ \min(x_j) & \text{if } x_j < 0 \,\forall j, \\ 0 & \text{otherwise,} \end{cases} \tag{2.10}$$

and θ a parameter between 1 and 2 [1].

For systems of equations the TVD property is not preserved. Nevertheless, the same choice is made for each vector component, and furthermore for each dimension in the multidimensional case.

The second order convergence of the method corresponds to the Lip' seminorm, which is specially suited for analizing convergence of conservative methods [5].

3 Kurganov Tadmor interface

In this section we explain our interface method. For simplicity we start with the one dimensional case. First assume that we choose to place our interface at a point x_I of a domain Ω. We label our subdomains to the left and right of x_I with the letters L and R respectively.

We discretize L using N points and R using M points, with $x^L_{N-1} = x_I = x^R_0$, as seen in figure 1; that is, in both grids we store information of our estimation of $\overline{u}(x_I, t)$.

[†] The *total-variation* TV is defined as $TV(v(t)) = \sum_j |v_{j+1}(t) - v_j(t)|$. The TVD property implies that $\frac{d}{dt} TV(v) \leq 0$.

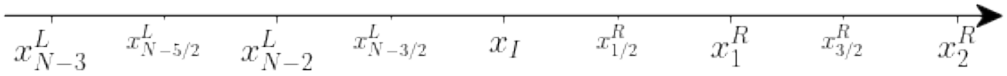

Figure 1: We split our domains in two regions L and R around an interface x_I, and discretize both regions so that they share a grid point at the interface. We mark our intermediate points for better understanding of the scheme.

Even though in the figure $\Delta x^L = \Delta x^R$, we will later see that that is not a necessary condition.

We recall that KT updates the estimated point averages of the solution at each grid point. The idea of our interface method is to use the points of the subgrids L and R to estimate only the left and right averages $v_I^L(t)$ and $v_I^R(t)$,

$$v_I^L(t) \approx \frac{1}{\Delta x^L}\int_{x^L_{N-3/2}}^{x_I} u(\xi,t)\,d\xi, \quad v_I^R(t) \approx \frac{1}{\Delta x^R}\int_{x_I}^{x^R_{1/2}} u(\xi,t)\,d\xi, \tag{3.1}$$

and latter communicate both grids by calculating the full average u_I,

$$v_I(t) \doteq \frac{\Delta x^L v_I^L(t) + \Delta x^R v_I^R(t)}{\Delta x^L + \Delta x^R} \approx \frac{1}{\Delta x^L + \Delta x^R}\int_{x^L_{N-3/2}}^{x^R_{1/2}} u(\xi,t)\,d\xi. \tag{3.2}$$

The way we achieve this is by setting to zero the derivative approximations, $(v_x)_I^L = (v_x)_I^R = 0$, as seen in figure 2. This way we avoid using information of the adjacent grid. Note that in this point the method is of first order. This is expected in interface methods as the number of grid points available decrease near the interface.

Our method then goes as follows. First we calculate the temporal derivatives of v_I^L and v_I^R,

$$\begin{aligned}
\frac{d}{dt}v_I^L &= -\frac{G_I^{L+} - G_I^{L-}}{\Delta x^L}, & \frac{d}{dt}v_I^R &= -\frac{G_I^{R+} - G_I^{R-}}{\Delta x^R},\\
G_I^{L+} &= f(v^{L+}_{I-1/2}) + a^L_{I-1/2} v^{L+}_{I-1/2}, & G_I^{R+} &= f(v^{R+}_{I+1/2}) - a^R_{I+1/2} v^{R+}_{I+1/2},\\
G_I^{L-} &= f(v^{L-}_{I-1/2}) + a^L_{I-1/2} v^{L-}_{I-1/2}, & G_I^{R-} &= f(v^{R-}_{I+1/2}) + a^R_{I+1/2} v^{R-}_{I+1/2}.
\end{aligned} \tag{3.3}$$

Note that for a given variable w we are using the notation $w^L_{I-1/2} = w^L_{N-3/2}$ and $w^R_{I+1/2} = w^R_{1/2}$. The values $v^{L\pm}_{I-1/2}$, $v^{R\pm}_{I+1/2}$, $a^L_{I-1/2}$ and $a^R_{I+1/2}$ are calculated using the definitions (2.6) and (2.7). Because $(v_x)_I^L = (v_x)_I^R = 0$, we also have $v^{L+}_{I-1/2} = v^{R-}_{I+1/2} = v_I$.

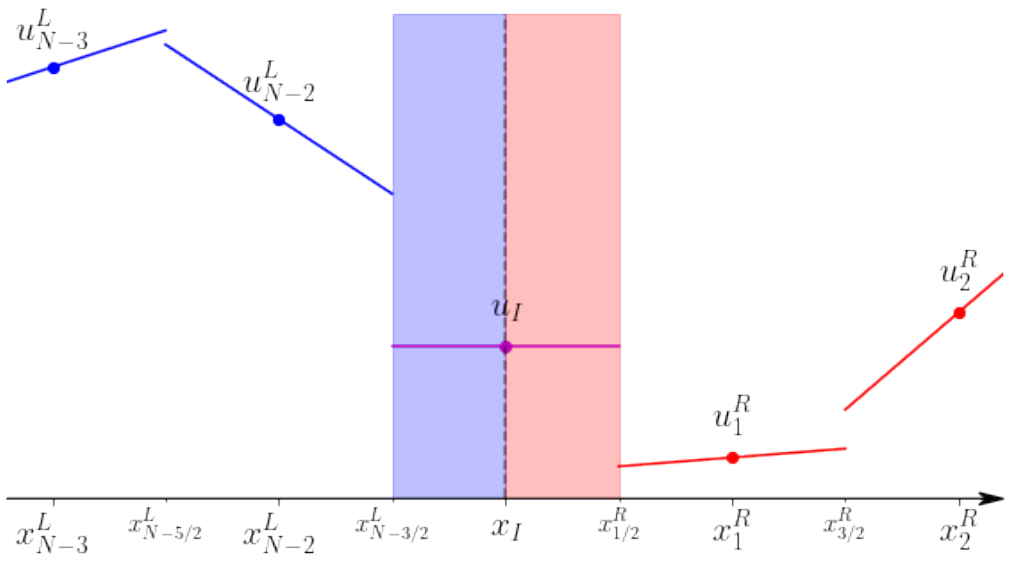

Figure 2: The interface is marked with a dashed line. For each point, we also plot a line of slope v_x. The left and right extremes of those lines correspond to the values $v^+_{j-1/2}$ and $v^-_{j+1/2}$ respectively. We mark in blue and red the averaging areas of v^L_I and v^R_I.

We now check that the TVD property still holds. From [1] and [4] we know that it is guaranteed if

$$\left|\frac{(v_x)_{j+1/2}}{\Delta v_j \pm 1/2}\right| \leq 2, \tag{3.4}$$

with $\Delta v_{j+1/2} = v_{j+1} - v_j$. This is clearly the case for our interface point, since $(v_x)_I = 0$.

After calculating the temporal derivatives, we integrate using our TVD temporal scheme to obtain v^L_I and v^R_I, and then update both values with the simple step

$$\begin{array}{rcl} v_I & = & \dfrac{\Delta x^L v^L_I + \Delta x^R v^R_I}{\Delta x^L + \Delta x^R} \\ v^L_I & \leftarrow & v_I \\ v^R_I & \leftarrow & v_I \end{array} \tag{3.5}$$

This way we essentialy recover the original second order Kurganov-Tadmor method, while maintaining ty. Although we could in theory approximate $(v_x)^L_I = \frac{v_I - v^L_{N-2}}{\Delta x^L}$ and $(v_x)^R_I = \frac{v^R_1 - v_I}{\Delta x^R}$, doing so does not guarantee that (3.4) holds.

As a final remark, we note that $\dfrac{dv^L_{I-1}}{dt}$ and $\dfrac{dv^R_{I+1}}{dt}$ are also slightly modified by our method, as they too use as information the value $(v_x)_I$. By the same arguments used before this modification does not alter the TVD condition neither.

As is the case with the full KT scheme, the extension of this method to systems of equations is done by implementing it to each vector component, and to each dimension in the multidimensional case.

4 Results

We present convergence results for one dimensional scalar equations, as well as results for the two dimensional Euler equation. In all cases we use the third order TVD Runge-Kutta scheme (3.3) from [3]. We set the parameter θ of (2.9) to 2 in the scalar cases and 1.5 for the Euler equation (see discussion of optimal θ values in [1]).

4.1 Advection

We consider the one dimensional advection equation in the domain $x \in [-2,2)$ with periodic boundary conditions

$$\frac{\partial}{\partial t}u(x,t) + \frac{\partial}{\partial x}u(x,t) = 0, \tag{4.1}$$

with smooth initial data corresponding to an eighth order polynomial peak,

$$u_0(x) = \begin{cases} (x-1)^4(x+1)^4 & \text{if } |x| < 1 \\ 0 & \text{if } |x| \geq 1. \end{cases} \tag{4.2}$$

For simplicity in the convergence analysis, we assume $\Delta x^L = \Delta x^R$. The solution to this problem is trivial and corresponds to $u(x,t) = u_0(x-t)$.

We evolve (4.1)-(4.2) until $T=20$, both with and whithout a numerical interface placed at $x_I = 0.5$. The evolution results are shown in figure 3a, and convergence results are shown in 3b for the seminorm Lip'. We fit the data with a power equation

$$||u - u_{exact}||_{Lip'} = b\Delta x^p. \tag{4.3}$$

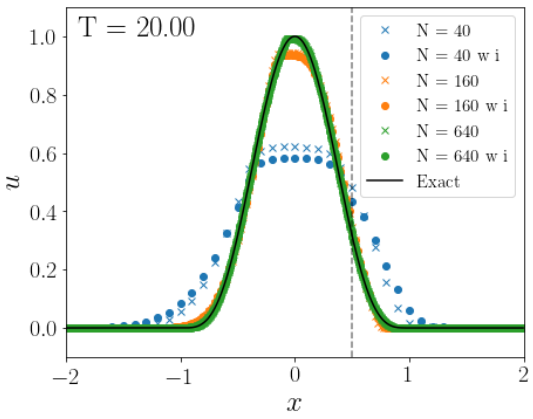

(a) Evolution of (4.2) for the advection equation with different number of points N and with (w i) and without interface.

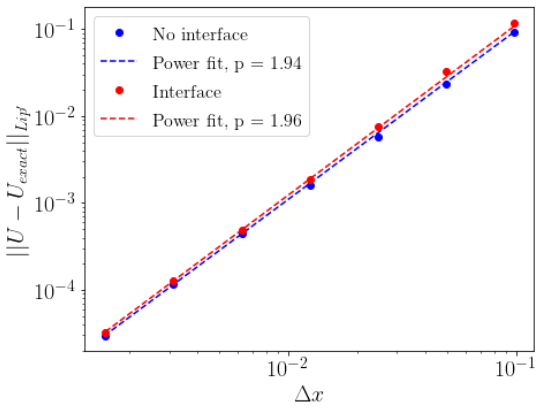

(b) Lip' convergence of (4.2) for the advection equation.

Figure 3: Results for the one dimensional advection problem at T = 20, corresponding to 4 periods. The CFL is set to 0.1 in all cases.

We notice that even though there is slightly greater numerical dissipation in the presence of interfaces, the second order global convergence is maintained.

4.2 Burgers equation

To study the behavior of shocks passing through the interface we consider now the one dimensional burgers equation

$$v_t + \left(\frac{v^2}{2}\right)_x = 0, \tag{4.4}$$

with smooth periodic initial data.

$$v(x,0) = 0.5 + \sin(x). \tag{4.5}$$

The solution of (4.5) is well known and develops a shock at time $T = 1$. Results of the second order convergence of the fully discrete KT scheme for this problem can be found in [1].

The convergence results are shown in the figure 5. We compare our results with a high resolution approximation using $N = 20480$ points without interface. As we can see, even the second order global convergence is maintained after the shock passes through the interface.

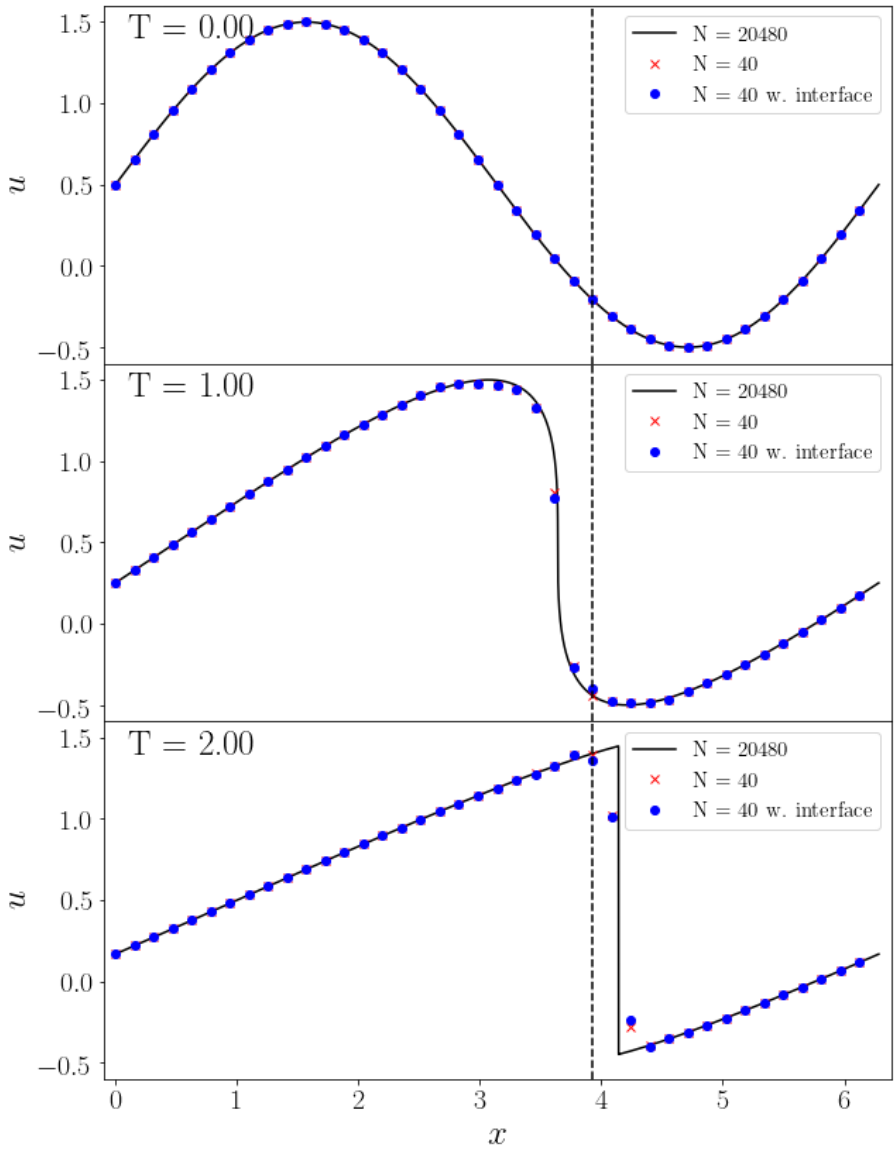

Figure 4: Evolution of (4.5) with the burgers equation at different times for $N = 40$ and $CFL = 0.1$ with and without an interface. The interface location is marked by the dashed black line.

We also continue the evolution up to $T = 114.0$, to allow the shock to travel through the interface several times. Results show that the second order convergence is maintained and can be seen in figures 6a and 6b.

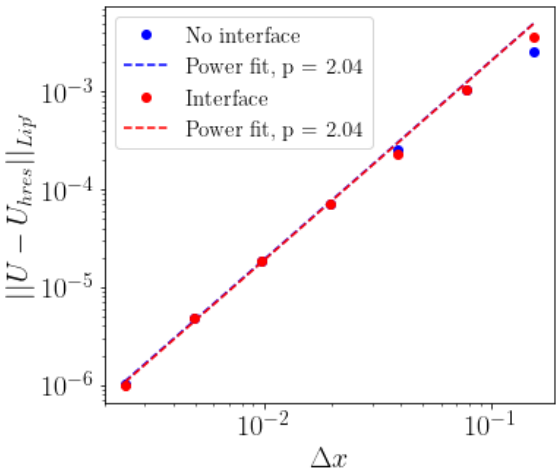

Figure 5: Convergence of (4.5) with the burgers equation at time $T = 2.0$ with CFL = 0.1. u_{hres} corresponds to the approximation with $N = 20480$.

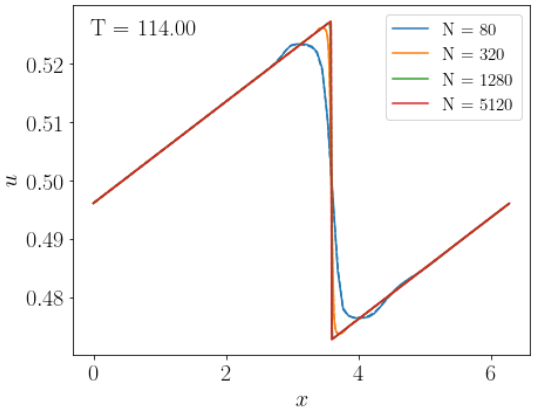

(a) Evolution of (4.5) with the burgers equation with different numbers of points N and with (dashed line) and without (continuous line) interface. This is after 10 passes of the shock across the interface.

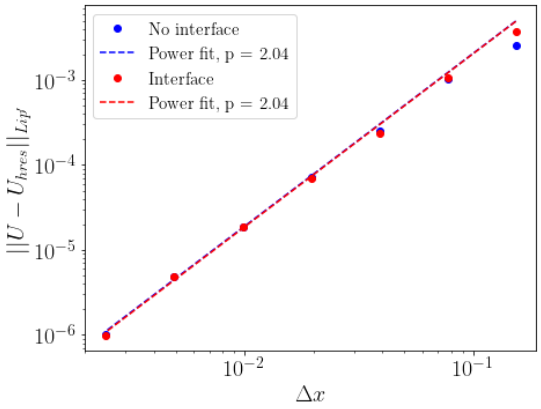

(b) Lip' convergence of (4.5) for the Burgers equation. u_{hres} corresponds to the approximation with $N = 20480$.

Figure 6: Results for the one dimensional Burgers problem at $T = 114$ and with $CFL = 0.1$.

4.3 Two dimensional Euler equation

We evolve the two dimensional Euler equations of gas dynamics [2],

$$\frac{\partial}{\partial t}\begin{pmatrix}\rho\\ \rho u\\ \rho w\\ E\end{pmatrix}+\frac{\partial}{\partial x}\begin{pmatrix}\rho u\\ \rho u^2+p\\ \rho uw\\ u(E+p)\end{pmatrix}+\frac{\partial}{\partial y}\begin{pmatrix}\rho u\\ \rho uw\\ \rho w^2+p\\ u(E+p)\end{pmatrix}=0, \tag{4.6}$$

where ρ is the density of the gas, (u,w) the 2D fluid velocity, E the energy of the system and p the pressure, which obeys the equation of state

$$E=\frac{1}{2}\rho(u^2+w^2)+\frac{p}{\gamma-1}, \tag{4.7}$$

with γ the ratio of specific heats. We use $\gamma=1.4$, which corresponds to an ideal gas.

4.3.1 Implosion

We consider the implosion problem from [6]. It consists of a box $(x,y)\in(-0{,}3,0{,}3)\times(-0{,}3,0{,}3)$ with reflective boundary conditions, with a smaller box inside rotated by $\pi/4$ with corners in $(\pm 0.15,0)$ and $(0,0.15)$. The fluid velocity is set to zero everywhere, and initial pressure and density are set at $\rho_i=0.125$ and $p_i=0.14$ in the inner box, and $\rho_o=1, p_o=0$ outside of it.

We take advantage of the symmetry of the problem and only evolve the upper right quadrant of the full domain, that is, $(x,y)\in(0,0.3)\times(0,0.3)$.

Results of the implementation of the method can be seen in figure 7. In figure 8 we show the difference between the approximation without interface and the approximations with one and two interfaces.

We find that shocks are correctly propagated through the interfaces even when not aligned with them, and there is no indication of bouncing effects. Most of the difference between approximations is located around shocks, and are a product of the greater numerical dissipation.

4.3.2 Gresho vortex

As a final test we evolve the Gresho vortex [6] in a box $(x,y)\in[-1,1)\times[-1,1)$:

$$u_\phi(r)=\begin{cases}5r\\ 2-5r\\ 0\end{cases}, p(r)=\begin{cases}5+\frac{25}{2}r^2 & 0\le r<0.2\\ 9+\frac{25}{2}r^2-20r+4\ln(5r) & 0.2\le r<0.4\\ 3+4\ln(2) & 0.4\le r\end{cases} \tag{4.8}$$

The exact solution of this problem is independent of time.

Results seen in figure 9 show that the vortex is maintained for small times, but is destroyed after a long evolution. This indicates that local instabilities are triggered across interfaces in this problem.

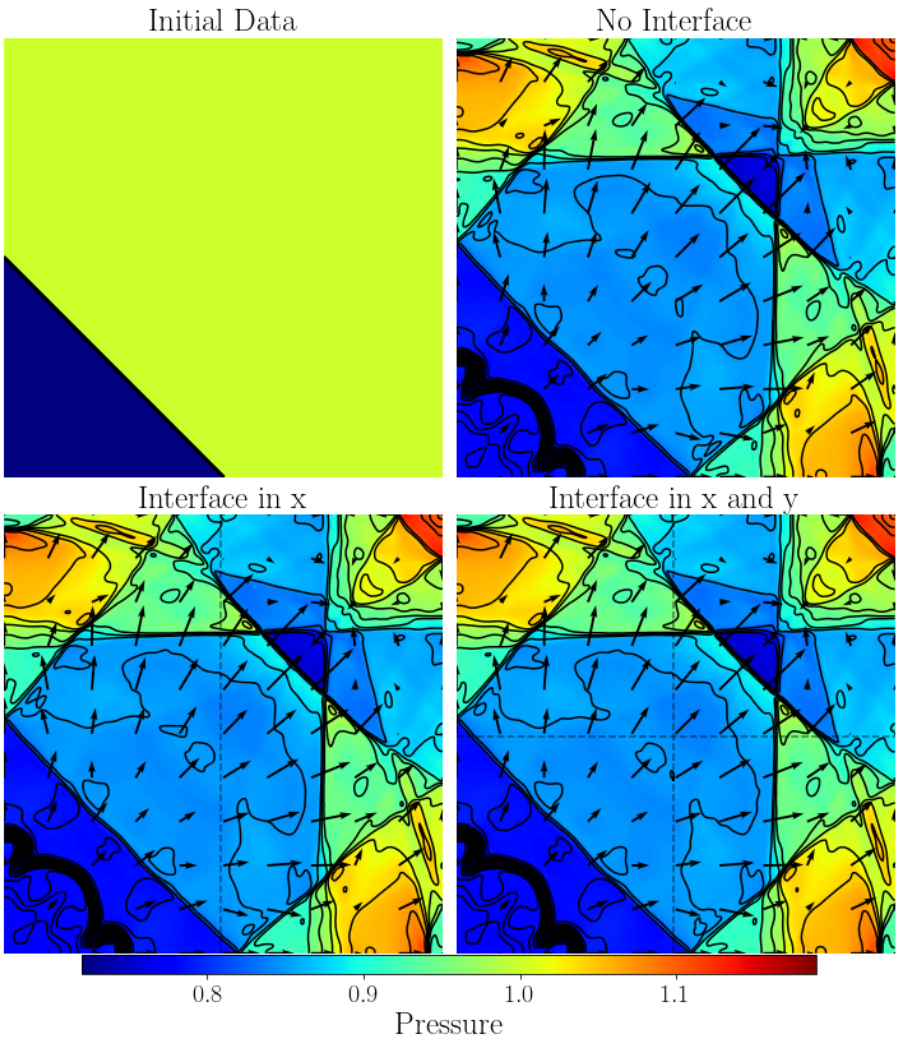

Figure 7: Implosion problem on a 400×400 grid with $CFL=0.1$ at $T=2.5$ with and without interfaces. Density contour lines and velocity arrows are overlaid over the pressure color maps.

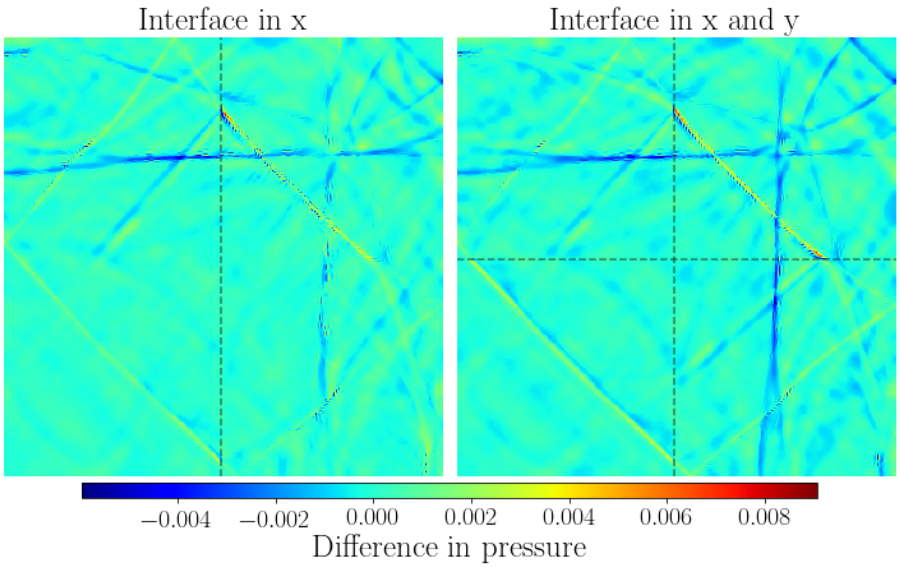

Figure 8: Difference between the approximations with and without interfaces for the implosion problem on a 400×400 grid with $CFL = 0.1$ at $T = 2.5$.

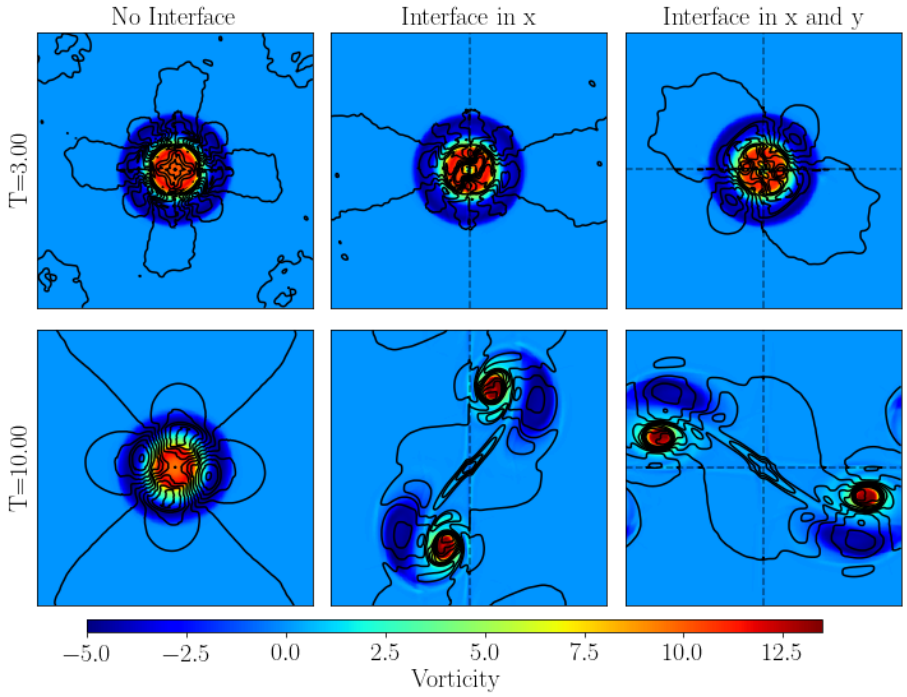

Figure 9: Gresho problem on a 400×400 grid with $CFL = 0.1$ at $T = 3.0$ and $T = 10.0$ with and without interfaces. Density contours are overlaid over the vorticity color maps.

5 Conclusions:

We introduced a simple TVD interface method for the implementation of a multiblock Kurganov-Tadmor semidiscrete scheme. We found that this method increases the numerical dissipation of the solution in the interface region, but maintains the global second order of convergence of the KT method in the one dimensional scalar case.

We also applied the method to the 2D Euler equations. We found that it allows the transmission of shock discontinuities without loss of phase or change in speed and regardless of the orientation of the shock with respect to the interface. Finally, we also found that instabilities are triggered across interfaces in the very demanding Gresho vortex problem. This is is not surprising since the interface method breaks the grid homogeneity and also increases the local dissipation.

References

[1] A. Kurganov and E. Tadmor, "New high-resolution central schemes for nonlinear conservation laws and convection–diffusion equations," *Journal of Computational Physics*, vol. 160, pp. 241–282, 05 2000.

[2] R. J. LeVeque, *Numerical Methods for Conservation Laws*. Birkhäuser Basel, 1992.

[3] S. Gottlieb and C.-W. Shu, "Total variation diminishing runge kutta methods," *Mathematics of Computation*, vol. 67, no. 221, pp. 73–85, 1998.

[4] S. Osher, "Convergence of generalized muscl schemes," *SIAM Journal on Numerical Analysis*, vol. 22, no. 5, pp. 947–961, 1985.

[5] S. S. U. S. Fjordholm, "Second-order convergence of monotone schemesfor conservation laws," *SIAM J. Numerical Analysis 54(3) (2016) 1920-1945.*, 2016.

[6] R. Liska and B. Wendroff, "Comparison of several difference schemes for the euler equations in 1d and 2d," in *Hyperbolic Problems: Theory, Numerics, Applications* (T. Y. Hou and E. Tadmor, eds.), (Berlin, Heidelberg), pp. 831–840, Springer Berlin Heidelberg, 2003.